Probing Neutrino Charge Radii with Coherent Elastic Solar Neutrino-Nucleus Scattering

O. Başlı[1,2], M. F. Mustamin[1], M. Demirci[1,*]

[1]*Department of Physics, Karadeniz Technical University, Trabzon, TR61080, Türkiye*

[2]*Department of Physics, Bursa Uludağ University, Bursa, TR16059, Türkiye*

Abstract

Coherent elastic neutrino–nucleus scattering (CEνNS), as a low-energy process within the Standard Model (SM), provides a powerful probe of neutrino electromagnetic properties, in particular the neutrino charge radius. Owing to its relatively large cross section, CEνNS is especially sensitive to such subleading effects. In this work, we investigate the impact of the neutrino charge radius on CEνNS induced by solar neutrinos. We calculate its contribution to the CEνNS cross section and derive constraints on the neutrino charge radius by analyzing current data from the CDEX-10 experiment. Our results are then compared with existing bounds reported in previous studies.

Keywords: CEνNS, solar neutrino, neutrino charge radius
DOI: 10.31526/PHEP.2025.08

1. INTRODUCTION

Neutrinos are commonly believed to be neutral particles, but in reality these can have a very small electric charge and are very likely to have a charge radius (see [1]). In the Standard Model (SM), the effective photon-neutrino interaction appearing as radiative corrections lead to a nonzero neutrino charge radius [2, 3, 4], which is intuitively related to the electromagnetic "size" of the neutrino [5]

$$\left\langle r^2_{\nu_\ell} \right\rangle_{\rm SM} = -\frac{G_F}{2\sqrt{2}\pi^2}\left[3 - 2\ln\left(\frac{m^2_\ell}{m^2_W}\right)\right]. \tag{1}$$

In this relation, m_ℓ is the mass of the charged lepton with flavor $\ell = e, \mu, \tau$ and m_W is the mass of the W gauge boson. Neutrino charge radius can be the most accessible neutrino electromagnetic property, because the SM predictions are only about one order of magnitude smaller than the experimental upper-limits. Numerical values of the neutrino charge radius are predicted by SM as [6, 7]

$$\begin{aligned}\left\langle r^2_{\nu_e} \right\rangle_{\rm SM} &= -8.3 \times 10^{-33}{\rm cm}^2 \\ \left\langle r^2_{\nu_\mu} \right\rangle_{\rm SM} &= -4.8 \times 10^{-33}{\rm cm}^2 \\ \left\langle r^2_{\nu_\tau} \right\rangle_{\rm SM} &= -3.0 \times 10^{-33}{\rm cm}^2\end{aligned} \tag{2}$$

for each flavor, respectively. Consequently, a measurement in a high-precision experiment that would be incompatible with these values would directly provide information about the physics beyond the SM (BSM). In BSM theories, neutrinos may also have flavor off-diagonal charge radius on a flavor basis, a so-called transition charge radius, which changes the neutrino flavor. Neutrino charge radius also has some effects on cosmology and astrophysical phenomena [8, 9].

Coherent elastic neutrino-nucleus scattering (CEνNS), theoretically predicted in 1974 [10], provides a powerful window for probing the neutrino charge radius. The CEνNS process was first observed by the COHERENT experiment in 2017 [11] at the Spallation Neutron Source, which is a neutral current weak interaction process of the SM. Relatively low-energy neutrinos in this process interact with a nucleus as a whole target. The coherence condition implies a very low momentum transfer. The CEνNS process provides a larger cross-section than the ones of other neutrino interactions at the same neutrino energy, and this scales with the square of the number of target neutrons (N^2). The N^2-dependence has been investigated by subsequent COHERENT measurements using different target materials such as argon [12] and germanium [13]. However, the expected signature of this process is a very low nuclear recoil energy, making it difficult to detect experimentally. Because it is well defined at low energies in the SM, the CEνNS is an interesting tool for probing the new physics effects from neutrino electromagnetic properties, light mediator models, astrophysics and nuclear structure.

The sun produces large neutrino fluxes; especially those from the ^{8}B solar neutrinos that meet the properties required to induce significant CEνNS events in direct detection (DD) dark matter (DM) experiments. These experiments are turning into excellent low-energy neutrino detectors. They are produced in the core of the sun by nuclear fusion reactions. Since CEνNS is particularly sensitive to low-energy neutrinos, utilization of solar neutrinos is an interesting framework for studying this process. The appearance of neutrino charge radius could alter the SM prediction of the process and thus can be tested using data from DD facilities. Probing this process in this way will complement the existing results from other experiments. The most stringent reported limits on the neutrino charge radius at DD experiments currently come from XENONnT with the lower limit being about two orders of magnitude larger than the SM prediction [14].

The CDEX-10 [15, 16] is one such DD experiment with ultra-low energy threshold pPCGe detectors. The experiment has a primary goal to research light DM candidates. In this context, the observation limits of the neutrino charge radius in the energy region of interest for the CEνNS process can be im-

*Corresponding author: mehmetdemirci@ktu.edu.tr

proved. We use the recent data of the CDEX-10 collaboration [17], which was carried out considering the flux of solar neutrinos. We place new allowed regions on the neutrino charge radius from both 1 degree of freedom (dof) and 2 dof analysis of the data and compare these with existing constraints from previous studies.

We organize the remainder of this work in the following. In Sec. 2, we review the analytical expression of the CEνNS in the SM and in the presence of a neutrino charge radius. In Sec. 3, we present the analysis procedure used for limit setting. In Sec. 4, we provide the analysis results for neutrino charge radius and compare these with previously available limits. Finally, in Sec. 5, we summarize our work.

2. ANALYTICAL CALCULATIONS

In this section, we present the differential cross-section expressions for the CEνNS process and the neutrino charge radius contribution in the SM.

In the SM, the differential cross-section of the neutrino with the initial energy E_ν scattering off the nucleus with the recoil energy T_{nr} is given by

$$\frac{d\sigma_{\rm SM}}{dT_{nr}}(E_\nu, T_{nr}) = \frac{G_F^2 m_{\mathcal{N}}}{\pi}\left(1 - \frac{m_{\mathcal{N}} T_{nr}}{2E_\nu^2}\right) \times \left[g_V^p Z F_Z(|\vec{q}|^2) + g_V^n N F_N(|\vec{q}|^2)\right]^2 \tag{3}$$

where $m_{\mathcal{N}}$ is the nucleus mass, and G_F is the Fermi constant. In Fig.1, the representative Feynman diagram is shown for this process. The process occurs as neutrino interacts with the nucleus as a whole. For the transfer momentum $|\vec{q}| \lesssim \frac{1}{R}$ with the typical size of nucleus R, the coherent scattering will give a cross-section enhancement. The neutron and proton vector couplings are given by

$$g_V^p = \frac{1}{2}(1 - 4\sin^2\theta_W) \quad \text{and} \quad g_V^n = -\frac{1}{2}, \tag{4}$$

respectively. We consider the value of $\sin^2\theta_W = 0.23863$ calculated in the minimal subtraction ($\overline{\rm MS}$) renormalization scheme at low momentum transfer [18]. Note that the cross-section of the process in the SM is obtained as flavor-independent at the tree level. There are flavor dependencies in the small loop corrections, however, they have no important effect on the current sensitivities [19]. The weak nuclear form factors are given by $F_Z(|\vec{q}|^2)$ and $F_N(|\vec{q}|^2)$, which describe the nucleon complex structure of the nuclei. The form factor is generally taken to be identical for both neutron and proton, namely $F_Z \simeq F_N = F$. For this treatment, we use the Helm parametrization [20].

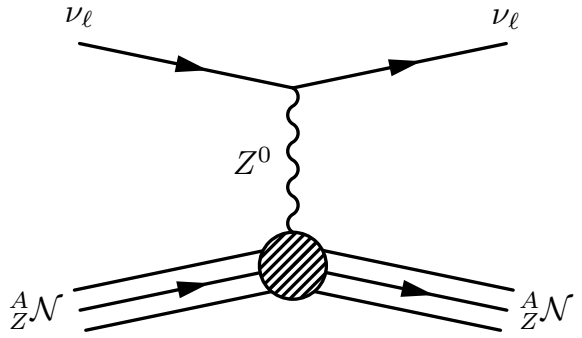

FIGURE 1: Feynman diagram of the CEνNS process.

The Lagrangian representing the electromagnetic interaction between the neutrino and the photon is written as [21]

$$\mathcal{L}_\ell^{em} = -ieF_Q(q^2)\bar{\nu}_\ell\gamma_\mu\nu_\ell A^\mu \tag{5}$$

where $F_Q(q^2)$ is the electrical form factor for neutrinos and A^μ is the photon field. In the CEνNS process, the matrix element for the contribution of the neutrino charge radius is taken as [4]

$$\mathcal{M} = \left[\frac{2\pi Z e^2}{3}\langle r_{\nu_\ell}^2\rangle \bar{u}(p_3)\gamma^\mu u(p_1)\right] j_\mu^{\mathcal{N}} \tag{6}$$

where $j_\mu^{\mathcal{N}} = (p_{2\mu} + p_{4\mu})F(|\vec{q}|^2)$, with p_2 and p_4 being the initial and final nuclear four-momenta. The neutrino charge radius contribution to the CEνNS process can also be obtained by substituting

$$\sin^2\theta_W \to \sin^2\theta_W\left(1 - \frac{\pi\alpha_{EM}}{3\sqrt{2}\sin^2\theta_W G_F}\left\langle r_{\nu_\ell}^2\right\rangle\right) \tag{7}$$

for the weak mixing angle in Eq.(4). In the BSM, the neutrino charge radius can also include flavor off-diagonal terms in the flavor basis. However, we will only consider the scenario including flavor diagonal terms.

3. DATA ANALYSIS DETAILS

In the recent CDEX-10 study [17], event rates of CEνNS along with neutrino-electron scattering have been published. The event rates of the process are calculated by integrating the neutrino flux with the cross-section. The corresponding nuclear recoil event is given by [22]

$$\frac{dR}{dT_{nr}} = N_T\int_{E_\nu^{min}}^{E_\nu^{max}} dE_\nu \frac{d\Phi(E_\nu)}{dE_\nu}\frac{d\sigma(E_\nu, T_{nr})}{dT_{nr}} \tag{8}$$

where $d\Phi(E_\nu)/dE_\nu$ is the differential neutrino flux. The factor of $N_T = m_t N_A/m_A$ indicates the number of target nucleus per unit mass of detector material. The minimum neutrino energy satisfies

$$E_\nu^{min} = T_{nr}\left(1 + \sqrt{1 + 2m_{\mathcal{N}}/T_{nr}}\right)/2 \tag{9}$$

while the maximum neutrino energy E_ν^{max} is taken as the end point of the solar neutrino flux. Furthermore, the maximum value of nuclear recoil energy is $T_{nr}^{max} = \frac{2E_\nu^2}{2E_\nu + m_{\mathcal{N}}}$. We consider solar neutrino flux from the BS05(OP) Standard Solar Model [23, 24]. There are eight neutrino fluxes produced from the pp chain and CNO cycle inside the sun. The neutrinos of the pp chain are produced from 5 nuclear reactions called *pp*, *pep*, hep,^{8}B, and ^{7}Be. Meanwhile, the neutrinos in the CNO cycle originate from decays of ^{13}N, ^{15}O, and ^{17}F.

As a result of oscillations [25, 26, 27], solar neutrinos arrive at a detector on Earth with a mixture of ν_e, ν_μ, and ν_τ. For each flavor, we consider the survival probabilities

$$\Phi_{\nu_e}^i = \Phi_{\nu_e}^{i\odot} P_{ee}, \tag{10}$$

$$\Phi_{\nu_\mu}^i = \Phi_{\nu_e}^{i\odot}(1 - P_{ee})\cos^2\vartheta_{23}, \tag{11}$$

$$\Phi_{\nu_\tau}^i = \Phi_{\nu_e}^{i\odot}(1 - P_{ee})\sin^2\vartheta_{23}. \tag{12}$$

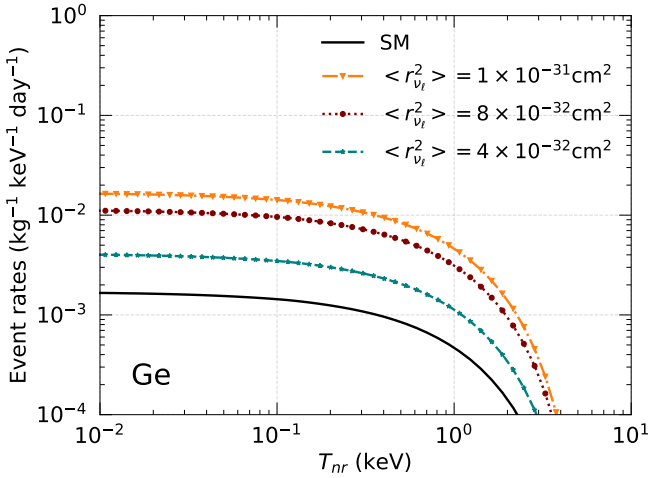

FIGURE 2: The predicted event rates of neutrino charge-radius contributions to CEνNS for various benchmark values.

The electron-neutrino flux from thermonuclear reactions in the core of the Sun is represented by $\Phi^{i}_{\nu_e}{}^{\odot}$, with $i = hep, {}^8\text{B}$. P_{ee} represents the ν_e survival probability on the Earth [28]. In our calculation, we take the day-night asymmetry because of the Earth's matter effect. We consider the normal ordering neutrino oscillation parameters from the 3-ν oscillation of NuFit-5.3 [29].

The recent CDEX-10 data on neutrino-nucleus scattering are presented in terms of electron-equivalent recoil energy. Therefore, it is converted into nuclear recoil energy using the Linhard quenching factor [30]

$$Y(T_{nr}) = \frac{\kappa g(\epsilon)}{1 + \kappa g(\epsilon)} \tag{13}$$

where $\kappa = 0.162$ and $g(\epsilon) = 3\epsilon^{0.15} + 0.7\epsilon^{0.6} + \epsilon$ with $\epsilon = 11.5Z^{-7/3}T_{nr}$. The value of κ is chosen to closely match the recent measurement in the low-energy interval [31, 32]. We notice that the Linhard formulation is suitable for relatively high nuclear recoil energy, namely $T_{nr} > 0.254$ keV. With the quenching factor, the nuclear recoil energy is converted into electron equivalent by using

$$T_{ee} = Y(T_{nr})T_{nr} \tag{14}$$

Thus, the differential rate as a function of the T_{ee} is calculated as

$$\frac{dR}{dT_{ee}} = \frac{dR}{dT_{nr}}\left[Y(T_{nr}) + T_{nr}\frac{dY(T_{nr})}{dT_{nr}}\right]^{-1} \tag{15}$$

We use the Gaussian approach of the χ^2 function [33] to derive constraints on the corresponding model parameters:

$$\chi^2 = \min_{(\alpha,\beta)}\left[\sum_{i=1}^{20}\left(\frac{R^i_{exp} - R^i_{obs}}{\sigma^i}\right)^2 + \left(\frac{\alpha}{\sigma_\alpha}\right)^2 + \left(\frac{\beta}{\sigma_\beta}\right)^2\right] \tag{16}$$

Here, R^i_{obs} and R^i_{exp} denote the measurement and theoretical event rates (consists of SM plus background plus new physics contributions) respectively, in the i-th energy bin. The experimental uncertainty is denoted by σ^i for the i-th energy bin. The χ^2 is minimized with respect to all nuisance parameters α and β which correspond to the ^{8}B and hep neutrino fluxes, respectively. The uncertainties of solar neutrino fluxes are denoted by σ_α for ^{8}B and σ_β for hep neutrino fluxes.

4. NUMERICAL RESULTS

In this section, we provide our analysis results. First, we plot the predicted event rate from contributions of the neutrino charge radius along with the predicted event rate of the SM CEνNS for the Ge target nuclei in Fig.2. Here, we set $\langle r^2_{\nu_\ell}\rangle$ for three different values. It is clear that the larger the charge radius the higher its contribution to the SM prediction. The constant spectrum can be seen in all the energy ranges. This is anticipated from Eq.(7) which has no dependency on recoil energy.

Figure 3 presents the 90% confidence level (C.L.) allowed contours for the neutrino charge radii parameter pairs obtained from the recent CDEX-10 dataset. The analysis was performed in the $\langle r^2_{\nu_e}\rangle - \langle r^2_{\nu_\mu}\rangle$, $\langle r^2_{\nu_e}\rangle - \langle r^2_{\nu_\tau}\rangle$, and $\langle r^2_{\nu_\mu}\rangle - \langle r^2_{\nu_\tau}\rangle$ planes, where all other electromagnetic properties were fixed to their SM values. We found $-128.09 \times 10^{-32}\,\text{cm}^2 \lesssim \langle r^2_{\nu_e}\rangle \lesssim 153.13 \times 10^{-32}\,\text{cm}^2$, $-223.37 \times 10^{-32}\,\text{cm}^2 \lesssim \langle r^2_{\nu_\mu}\rangle \lesssim 248.79 \times 10^{-32}\,\text{cm}^2$, and $-191.73 \times 10^{-32}\,\text{cm}^2 \lesssim \langle r^2_{\nu_\tau}\rangle \lesssim 217.13 \times 10^{-32}\,\text{cm}^2$. In all cases, the SM prediction (denoted by the white cross) remains well contained within the 90% C.L. allowed regions, with no discernible deviations observed. The resulting contours exhibit approximate elliptical symmetry and similar spatial extent across all parameter spaces, implying no significant degeneracy or correlation between individual charge radii components at the current experimental sensitivity. This indicates that the present CDEX-10 data constrains each neutrino flavor's effective charge radius to a comparable degree. Moreover, the absence of notable distortions or elongations in the contours suggests minimal parameter interdependence within the probed region.

These findings provide competitive and complementary constraints relative to existing direct detection limits on neutrino charge radii, obtained via low-energy neutrino-electron scattering. Recent work [34] has performed a combined analysis of data from PandaX-4T, XENONnT, and LZ. The results presented in [34] are follows $-99.5 \times 10^{-32}\,\text{cm}^2 \lesssim \langle r^2_{\nu_e}\rangle < 12.8 \times 10^{-32}\,\text{cm}^2$ and $-82.2 \times 10^{-32}\,\text{cm}^2 \lesssim \langle r^2_{\nu_{\mu/\tau}}\rangle < 88.7 \times 10^{-32}\,\text{cm}^2$. Our current results show few times less stringent bounds than these previous results. This difference that can be estimated comes from the different technology implemented, where the CDEX-10 applies germanium detector while the other DD experiments focus on noble-gas detector. While no statistically significant indication of BSM effects is observed, the achieved bounds affirm the capability of low-threshold dark matter detectors, such as CDEX-10, to effectively probe subleading neutrino electromagnetic properties and contribute to the global constraint landscape in this sector.

5. CONCLUSION

We have studied the contribution of neutrino charge radius to the CEνNS process with solar neutrino. In the SM, the neutrino charge radius is the only electromagnetic property of the neutrino that can have a nonzero value. It has interference with SM CEνNS, its contribution and the interference term are obtained by analytical calculations. The event rates of the process are obtained by convoluting solar neutrino flux with the cross-section. For the analysis, we considered recent CDEX-10 data. In doing so, the nuclear recoil energy is converted into electron-equivalent energy with the use of the Linhard quenching factor.

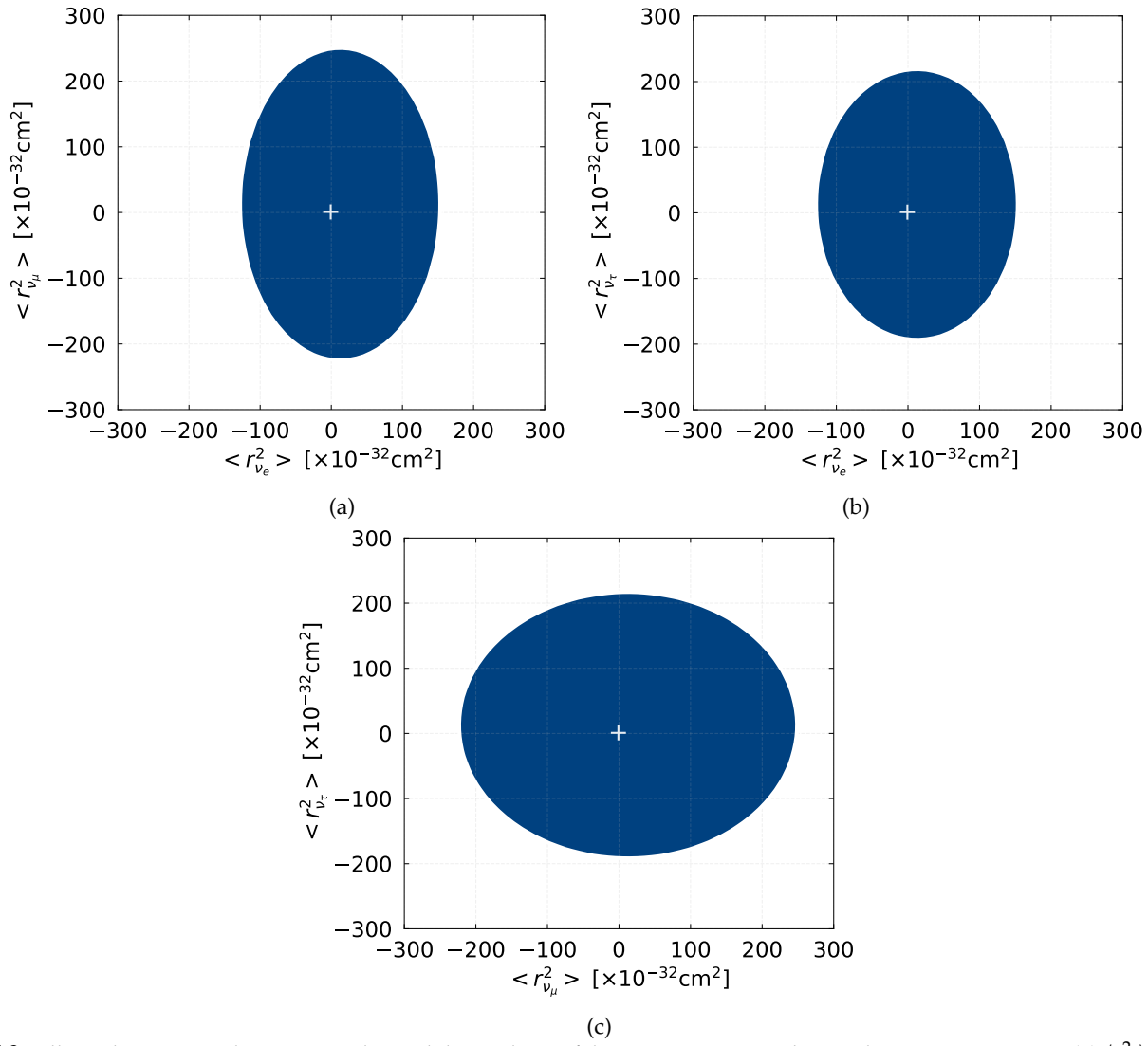

FIGURE 3: Allowed regions at the 90% C.L. derived the analysis of the recent CDEX-10 data in the parameter spaces (a) $\langle r^2_{\nu_e}\rangle - \langle r^2_{\nu_\mu}\rangle$, (b) $\langle r^2_{\nu_e}\rangle - \langle r^2_{\nu_\tau}\rangle$, and (c) $\langle r^2_{\nu_\mu}\rangle - \langle r^2_{\nu_\tau}\rangle$. The plus symbol denotes the SM values in Eq. (2).

We have shown our obtained limit of neutrino charge radius with 2 dof (90% C.L.). We have discussed our results with the allowed regions derived from other DD experiments. Our results for the neutrino charge radius are in compliance with the reactor and accelerator results. Our results could be utilized to study new physics signals, particularly for neutrino electromagnetic properties, by current and future experiments.

CONFLICTS OF INTEREST

The author declares that there are no conflicts of interest regarding the publication of this paper.

ACKNOWLEDGMENTS

We would like to thank the organizers of the International Conference on Neutrinos and Dark Matter 2024, dedicated to the memory of Prof. Dr. Durmuş Ali Demir, for the successful conference. This work was funded by the Scientific and Technological Research Council of Türkiye (TUBITAK) with the project 123F186.

References

[1] C. Giunti and A. Studenikin, Rev. Mod. Phys. 87, 531 (2015).
[2] J. Bernstein, T. D. Lee, Phys. Rev. Lett., 11(11), 512, 1963.
[3] W. A. Bardeen, R. Gastmans, B. Lautrup, Nucl. Phys. B, 46(1), 319-331, 1972.
[4] C. Giunti, K. A. Kouzakov, Y.-F. Li, A. V. Lokhov, A. I. Studenikin, S. Zhou, Ann. Phys. (Berlin), 528(1-2), 198-215, 2016.
[5] K. Fujikawa, B. W. Lee, A. I. Sanda, Phys. Rev. D, 6(10), 2923, 1972.
[6] K. Fujikawa, R. Shrock, Phys. Rev. D, 69(1), 013007, 2004.
[7] J. Papavassiliou, J. Bernabeu, D. Binosi, J. Vidal, Eur. Phys. J. C, 33, 865-867, 2004.

[8] A. D. Dolgov, and Y. B. Zeldovich, Rev. Mod. Phys. 53, 1 (1981).
[9] T. Altherr, and P. Salati, Nucl.Phys. B421, 662 (1994).
[10] D. Z. Freedman, Phys. Rev. D 9 (1974) 1389–1392.
[11] D. Akimov et al. [COHERENT Collaboration], Science, 357(6356), 1123-1126, 2017.
[12] D. Akimov et al. [COHERENT Collaboration], Phys. Rev. Lett., 126(1), 012002, 2021.
[13] S. Adamski et al., arXiv:2406.13806 [hep-ex].
[14] A. N. Khan, Phys. Lett. B **837** (2023), 137650.
[15] K. J. Kang et al. [CDEX], Front. Phys. (Beijing), 8, 412-437, 2013.
[16] H. Jiang et al. [CDEX], Phys. Rev. Lett. 120(24), 241301, 2018.
[17] X. P. Geng et al. [CDEX], Phys. Rev. Lett. 107(11), 112002, 2023.
[18] R. L. Workman et al. [Particle Data Group], Prog. Theor. Exp. Phys., 2022(8), 083C01, 2022.
[19] O. Tomalak, P. Machado, V. Pandey, R. Plestid, J. High Energ. Phys., 2021(02), 1-42, 2021.
[20] R. H. Helm, Phys. Rev., 104(5), 1466-1475, 1956.
[21] P. Salati, Astroparticle Physics, 2(3), 269–290, 1994.
[22] M. Demirci, M. F. Mustamin, Eur. Phys. J C, 85(1), 1, 2025.
[23] J. N. Bahcall, A. M. Serenelli, ApJ, 626(1), 530, 2005.
[24] J. N. Bahcall, A. M. Serenelli, S. Basu, ApJ, 621(1), L85-L88, 2005.
[25] Y. Fukuda et al. [Super-Kamiokande], Phys. Rev. Lett., 82(13), 2644, 1999.
[26] Q. R. Ahmad et al. [SNO Collaboration], Phys. Rev. Lett., 89(1), 011301, 2002.
[27] K. Eguchi et al. [KamLAND Collaboration], Phys. Rev. Lett., 90(2), 021802, 2003.
[28] M. Maltoni and A. Y. Smirnov, Eur. Phys. J. A **52** (2016) no.4, 87.
[29] I. Esteban, M. C. Gonzalez-Garcia, M. Maltoni, T. Schwetz, and A. Zhou, J. High Energ. Phys **2020**, 178 (2020).
[30] J. Lindhard, V. Nielsen, M. Scharff, P. V. Thomsen, Mat. Fys. Medd. Dan. Vid. Selsk 33(10), 1-42, 1963.
[31] A. Bonhomme et al., Eur. Phys. J. C, 82(9), 815, 2022.
[32] T. Schwemberger, T. T. Yu, Phys. Rev. D, 106(1), 015002, 2022.
[33] G. L. Fogli, E. Lisi, A. Marrone, D. Montanino and A. Palazzo, Phys. Rev. D, 66(5), 053010, 2002.
[34] C. Giunti, C. A. Ternes, Phys. Rev. D 108(9), 095044, 2023.